



Organic samples produced by ion bombardment of ices for the EXPOSE-R2 mission on the International Space Station



G.A. Baratta^{a,*}, D. Chaput^b, H. Cottin^c, L. Fernandez Cascales^a, M.E. Palumbo^a, G. Strazzulla^a

^a INAF-Osservatorio Astrofisico di Catania, via Santa Sofia 78, 95123 Catania, Italy

^b Centre National d'Etudes Spatiales (CNES), Centre Spatial de Toulouse, 18 Av. Edouard Belin, 31401 Toulouse Cedex 9, France

^c Laboratoire Interuniversitaire des Systèmes Atmosphériques (LISA), UMR CNRS 7583, Université Paris Est Créteil et Université Paris Diderot, Institut Pierre Simon Laplace, France

ARTICLE INFO

Article history:

Received 19 January 2015

Received in revised form

31 July 2015

Accepted 17 August 2015

Available online 28 August 2015

Keywords:

Astrobiology

Astrochemistry

Comets: general

Molecular processes

Method: laboratory

Techniques: spectroscopic

ABSTRACT

We describe the preparation and characterization (by UV–vis–IR spectroscopy) of a set of organic samples, stable at room temperature and above, that are part of the experiment “Photochemistry on the Space Station (PSS)” planned to be enclosed in the EXPOSE-R2 mission, which will be conducted on the EXPOSE-R facility. The core facility is placed outside the International Space Station (ISS) on the Universal Platform D (URM-D platform) of the Russian module Zvezda. The organic materials are prepared in the Catania laboratory after 200 keV He⁺ irradiation of icy mixtures, namely N₂:CH₄:CO deposited at 16 K on MgF₂ windows furnished by the European Space Agency. It is widely accepted that such a kind of materials produced by energetic processing are representative of organic material in some astrophysical environments as comets. Once expelled from comets these materials are exposed to solar radiation during their interplanetary journey before they eventually land on Earth and other planetary objects where they might give a contribution to the chemical and pre-biogenic evolution. In particular our residues contain different chemical groups, including triple CN bonds that are considered relevant to pre-biotic chemistry. Therefore the samples will be exposed, for several months, to the solar ultraviolet photons that are a major source of energy to initiate chemical evolution in the solar system. This will allow analysis of their destruction or modification and evaluation of their lifetime in the interplanetary medium. The samples have three different thicknesses that will allow estimation of the depth profile of destruction. This experiment overcomes the limits of ground tests which do not reproduce exactly the space parameters.

© 2015 Elsevier Ltd. All rights reserved.

1. Introduction

Earth atmosphere absorbs all the ionizing (below 125 nm) and most of the still harmful (below 310 nm) solar UV photons. The solar UV domain is crucial for the organic chemistry since it is the one driving most of the chemical evolution via photochemical reactions in the solar system (Cottin et al., 2015a). Samples mounted outside the International Space Station (ISS) can be exposed to the unfiltered solar electromagnetic spectrum.

Considering the solar standard spectrum for space application ASTM-E-490 (<http://www.astm.org/Standards/E490.htm>, <http://rredc.nrel.gov/solar/spectra/am0/>), we obtain an integral FUV flux (119.5 < λ < 206.7 nm) i.e. for E_{photons} > 6 eV of: F_{solar}(UV) =

1.54×10^{13} photons cm⁻² s⁻¹ at 1 AU, in agreement with the flux of 1.5×10^{13} photons cm⁻² s⁻¹ given by Cottin et al. (2015a) over the 120–200 nm range. In this paper we describe the preparation and the characterization of organic samples that will be exposed to solar electromagnetic radiation for several, between 12 and 18, months on board of the ISS. The used facility will be the ESA (European Space Agency) EXPOSE-R, placed outside the ISS on the Universal Platform D (URM-D platform) of the Russian module Zvezda and used to perform long term exposures. The EXPOSE-R2 mission (2014) uses the core facility of previous missions (EXPOSE, EXPOSE-R) (Cottin et al., 2015a, 2015b; Vigier et al., 2013 and references therein). It will accommodate several chemical and biological Russian and European experiments among which the PSS (Photochemistry on the Space Station). The exposure of the organic materials here discussed is part of the PSS experiment and has an astrobiological relevance being aimed at evaluating the

* Corresponding author. Tel.: +39 0957332313.

E-mail address: gbaratta@oact.inaf.it (G.A. Baratta).

evolution of organic molecules and at measuring to what extent some chemical, biological or biochemical samples are resistant to long term exposure to the space environment. Laboratory studies are carried out with the aim to simulate the photolysis of organics in different astrophysical environments. These studies use different kinds of UV sources in the vacuum UV (VUV) range ($100 < \lambda < 200$ nm) in order to simulate the cosmic UV radiation field. Nevertheless none of the used UV sources is able to accurately reproduce the solar VUV spectrum (Cottin et al., 2015a). In particular it has been observed that differences of a factor 10 or even > 100 in the photolysis kinetic exist between the extrapolation of laboratory results to space condition and the measurements obtained for low Earth orbit exposed organic samples (Guan et al., 2010). Hence trough experiments conducted in space it is possible to expose samples to the real UV solar spectrum, the results can be extrapolated to various astrophysical environments and are very accurate for the solar system.

The organic materials that our group has prepared have been synthesized by energetic ion bombardment of icy mixtures (N_2 : CH_4 : CO) deposited on MgF_2 windows at 16 K. The chosen ice mixtures are well representative of ices present on the surfaces of Trans Neptunian Objects (TNO) and of comets in the Oort cloud. In fact TNOs (e.g. Pluto) exhibit surface spectral features attributed to several species, among which solid nitrogen, methane and carbon monoxide (e.g. Owen et al., 1993). Water ice is also observed on the surface of some objects and it is thought to be present in the underneath layers of all of the objects. Its observation is restrained or inhibited by the presence of dark materials that could be the result of cosmic ion bombardment of surface ices as suggested since a long time on the base of simulation experiments similar to those here described (Grundy and Buie, 2002; Brunetto et al., 2006). Also comets in the Oort cloud are rich in C, N, and O, bearing icy molecules and could have developed a thick organic crust. Once formed and expelled from the solar system in the Oort cloud, comets have been exposed to the flux of galactic cosmic rays (GCR). In particular it has been estimated that the external (0.1–0.5 m) layers of a comet in the Oort cloud were subjected, in 4.6×10^9 yr, to an irradiation dose of 600 eV/16 u (e.g. Strazzulla and Johnson, 1991). Deeper layers were subjected to a lower dose because the most abundant but less energetic ions are stopped by the external layers. It has been suggested that a comet exposed to background particle irradiation in the Oort cloud develops a substantial crust (e.g. Strazzulla and Johnson, 1991) under which water ice remains the dominant species. Although the dose at depth is less than that suffered in the early evolutionary phases (e.g. Strazzulla and Baratta, 1992), it could be relevant in producing chemical modification in the irradiated ices. The development of an organic crust due to the conversion of low molecular weight hydrocarbons into a refractory organic residue occurs on a dosage scale of the order of 100 eV/16 u (Strazzulla and Johnson, 1991). Due to the solar modulation, present models suggest maximum irradiation dose far from the sun in the local interstellar medium (LISM) (Cooper et al., 2003). In particular it has been shown that on time scales of the order of the age of the solar system, an outer web of devolatilized material, corresponding to a dosage of 100 eV/16 u, is developed down to substantial depths, especially for comets in the Oort clouds, but also for scattered TNOs and marginally for classical Kuiper's objects (Strazzulla et al., 2003). Also UV processed ices could be present in comets. It has been shown that for interstellar grains in dense region, the energy released by cosmic UV photons is about one order of magnitude greater than that released by cosmic ray particles in the ice grain mantles so that, from the energy input point of view, the cosmic-ray induced UV field is more important for the chemistry in the ice mantles (Shen et al., 2004). On the other hand, the penetration depth of UV photons in ices is on the order of 0.15 μm (Jenniskens

et al., 1993); hence the amount of UV processed external ice layers of a comet or a TNO is negligible with respect to the 0.1–0.5 m layer depth altered by galactic cosmic rays at a significantly high dose. Nevertheless comets forms in the outer part of the solar nebula where temperature remained low enough so that interstellar grains could have survived. Hence UV processed organic materials could have been incorporated in comets.

When comets that originates both from the Kuiper belt (i.e. the TNOs region) and from the Oort cloud arrive in the proximity of the Sun (~ 3 AU) the water dominated sublimation expels gas and dust. The presence of supervolatiles, such as, CO , CO_2 , N_2 , CH_4 , etc., also plays a key role in cometary activity. Unlike water ice, they may sublime at much larger heliocentric distances; up to 25 AU (e.g., Szabó et al., 2011). This governs cometary activity well behind the water ice frost line (~ 3 AU). As a component of the dust there are solid refractory organic materials thought to be analogous to those synthesized in laboratory experiments similar to those here discussed. These materials travel the interplanetary medium where they are exposed to the radiation (cosmic rays, solar ion populations, solar photons), before to be eventually delivered on the surface of the Earth and all of the other objects in the solar system.

As detailed below, the organic residues contain different chemical groups, including triple $C \equiv N$ bonds that are considered relevant to pre-biotic chemistry (e.g. Palumbo et al., 2000a, 2000b). Laboratory experiments show that the $C \equiv N$ bonds are permanent at room temperature, but are destroyed by further irradiation (Palumbo et al., 2004). Their exposure to interplanetary space environments in the EXPOSE-R2 facility on board ISS will allow analysis of their destruction or modification and evaluation of their lifetime in the interplanetary medium.

2. Preparation and in situ characterization

2.1. Ion irradiation chamber

The experimental apparatus used to irradiate frozen ices is the up-grading of that described many times (e.g. Strazzulla et al., 2001). It consists of a stainless steel ultrahigh-vacuum chamber operating at a pressure kept lower than 10^{-9} mbar, interfaced with a FTIR Bruker-Vertex 70 spectrometer ($10,000$ – 400 $cm^{-1} = 1$ – 25 μm) through IR transparent windows. Inside the vacuum chamber MgF_2 windows (furnished by ESA) are placed in thermal contact with a cold finger, whose temperature can be varied between 16 and 300 K (Fig. 1). A gas mixture N_2 : CH_4 : CO (1:1:1) is prepared in a separate mixing chamber that has previously been evacuated at a pressure lower than 10^{-6} mbar. 30 mbar of each species is introduced in the mixing chamber and then a needle valve is used to admit the gas mixture into the main chamber, where it freezes onto the MgF_2 window whose temperature has been fixed to 16 K. After deposition the samples have been irradiated by 200 keV He^+ ions. We have chosen to use a beam current density of about 2×10^{-1} $\mu A cm^{-2}$ a value that excludes the possibility of a macroscopic heating of the sample. The ion current is continuously measured during irradiation and integrated over time in order to have a continuous measurement of the ion fluence. We stopped the experiments when the total energy released by impinging ions to each of the 30 samples (dose, as usual given in eV/16 u, where u is the unified atomic mass unit defined as 1/12 of the mass of an isolated atom of carbon-12) was about 110 ± 5 eV/16 u. This value has been obtained by using the stopping power (eV/ μm) of 200 keV He^+ ions in the irradiated mixtures as calculated by the SRIM software (Ziegler et al., 2008). In all of the experiments the thickness of the sample is smaller than the penetration depth of the ions.

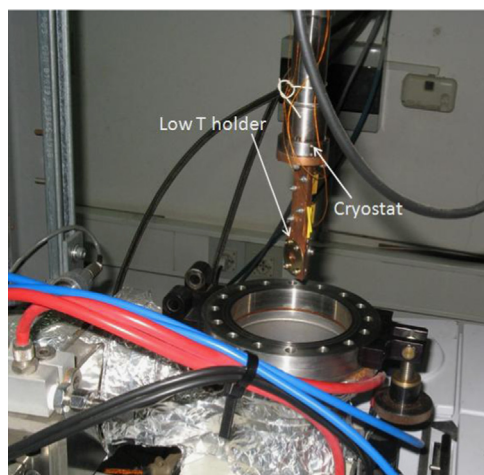


Fig. 1. The holder where the MgF₂ windows are fitted is at the end of a cryostat whose temperature can be varied between 16 and 300 K.

2.2. The properties of the deposited mixtures

The thickness of the layers has been monitored during deposition by using the routine technique of the interference fringe curve of a reflected He–Ne laser beam (see e.g. Baratta and Palumbo, 1998; Fulvio et al., 2009; Modica and Palumbo, 2010). As said we have prepared a total of 30 samples having three different thicknesses (10 samples for each thickness). The average values of the three thicknesses are: 1.322 ± 0.02 , 0.889 ± 0.01 and 0.456 ± 0.01 μm that correspond, in our experimental conditions, to interference curves exhibiting about 6, 4, and 2 fringes respectively.

At the end of deposition the FTIR spectra of the samples have been obtained. The sample plane forms an angle of 45° with the infrared beam and the ion beam. Examples of the obtained spectra (one for each thickness) are shown in Fig. 2.

The bottom panel in Fig. 2 exhibits the spectrum of the thickest sample (corresponding to 6 fringes in the laser interference curve). The presence of the CO band at ~ 2140 cm^{-1} and of two bands of CH₄ at ~ 3010 and ~ 1300 cm^{-1} is clear. In the other three panels these three bands are shown in detail for the three different thicknesses. It is important to say that the deposited nitrogen, being a symmetric, homo-nuclear species has not active IR band. However in the solids phase, due to the interaction with the neighboring molecules, the symmetry is broken and a very weak band appears at 2328 cm^{-1} . It has been shown that the strength of the band is extremely sensitive to the composition of the ice, in particular it is strongly enhanced relative to that of pure N₂ ice when NH₃, H₂O, or CO₂ are present, but it is almost unaffected by the presence of CO, CH₄, or O₂ (Sandford et al., 2001). The 2328 cm^{-1} band is not visible in the spectra of the as deposited samples. The spectra shown in Fig. 2 are ratiomed to the spectrum of the background acquired before deposition. All the spectra in the present paper are taken at a resolution of 1 cm^{-1} . If not differently said, each spectrum is plotted on an optical depth scale using the relation $I = I_0 \cdot e^{-\tau}$ (Beer–Lambert law), where $\tau = \alpha \cdot x$ (α is the absorption coefficient and x is the path length through the material). The column density of a given species is obtained using the equation:

$$N = \left(\int \tau(\nu) d\nu \right) / A$$

where N represents the column density (in molecules cm^{-2}), A represents the band strength (in cm molecule^{-1}), and $\int \tau(\nu) d\nu$ represents the area (in cm^{-1}) of a given band. It has been shown

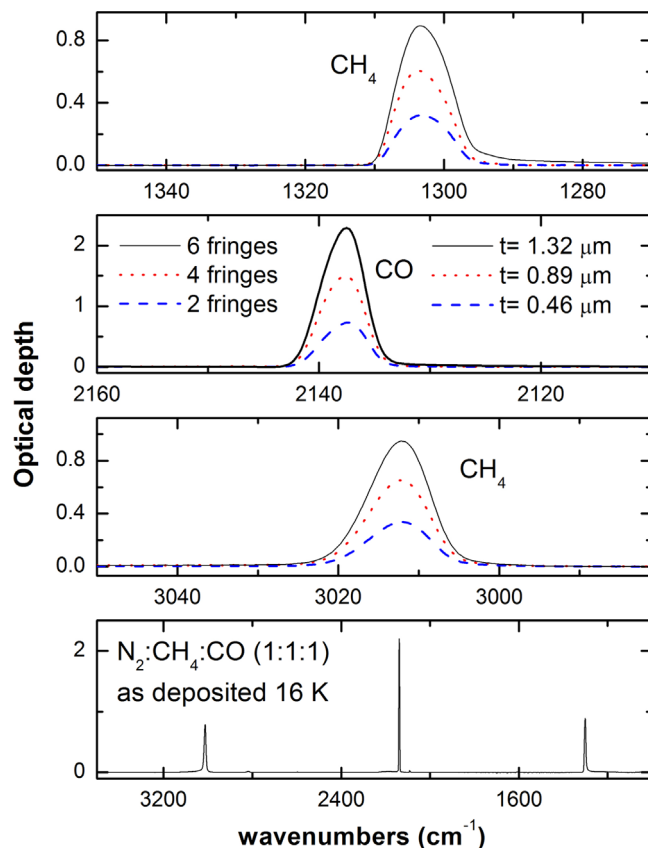


Fig. 2. Infrared spectra of the icy mixtures N₂:CH₄:CO (1:1:1) as deposited at 16 K on MgF₂ windows.

Table 1

Band strength values of reference. The CH₂N₂ solid-phase band strength is unavailable in the literature; the value given in the table has been derived from the gas phase integrated band strength.

Species	Peak position (cm ⁻¹)	Band strength (cm ² molecule ⁻¹)	Reference
CH ₄	3010	9.5×10^{-18}	Mulas et al. (1998)
CO	2140	1.1×10^{-17}	Jiang et al. (1975)
CO ₂	2340	7.6×10^{-17}	Yamada and Person (1964)
OCN ⁻	2167	4.0×10^{-17}	Demyk et al. (1998)
CH ₂ N ₂	2090	1.0×10^{-17}	from Raulin et al. (1995) (gas phase)
HCN	2090	5.1×10^{-18}	Bernstein et al. (1997)
HNCO	2262	7.2×10^{-17}	van Broekhuizen et al. (2004)

that the 1300 cm^{-1} band strength of CH₄ changes, due to matrix effects (see Kerkhof et al. (1999)), when CH₄ is diluted in a mixture, for this reason in the next we use only the 3010 cm^{-1} band to compute the CH₄ column density. Table 1 lists the band strength values used in this work.

The column densities of CO and CH₄ measured for the as deposited mixtures are reported in Table 2. As said, 10 samples have been prepared for each of the three thicknesses. In Table 2 the minimum, the maximum and the average value of the column density measured for each band are given along with the standard deviation. We can notice that the column densities of the samples having the same thickness are quite well reproducible as expected. Being the column densities of methane obtained by the ~ 3010 cm^{-1} band quite similar to those of CO and being the prepared gas mixture N₂:CH₄:CO (1:1:1), we assume that each of

Table 2
Column densities (see the text).

		Min value	Max value	Mean	Standard deviation
<i>As deposited (16 K) ($\times 10^{17}$ molecule cm^{-2})</i>					
2 fringes	CH ₄ (3010 cm^{-1})	3.3	3.7	3.4	0.1
	CO	2.5	3.6	3.2	0.3
4 fringes	CH ₄ (3010 cm^{-1})	5.8	6.4	6.1	0.2
	CO	5.6	6.6	6.1	0.4
6 fringes	CH ₄ (3010 cm^{-1})	8.4	9.4	9.0	0.3
	CO	7.5	9.8	9.1	0.6
<i>After irradiation (110 eV/16 u) ($\times 10^{17}$ molecule cm^{-2})</i>					
2 fringes	CO	1.02	1.48	1.21	0.14
	CO ₂	0.12	0.16	0.13	0.01
	OCN ⁻	0.04	0.07	0.06	0.01
	HCN, CH ₂ N ₂	1.02	1.34	1.16	0.11
	HNCO	0.15	0.18	0.16	0.01
4 fringes	CO	2.72	3.46	3.18	0.21
	CO ₂	0.31	0.38	0.35	0.02
	OCN ⁻	0.12	0.14	0.13	0.01
	HCN, CH ₂ N ₂	2.40	2.82	2.59	0.14
	HNCO	0.36	0.39	0.37	0.01
6 fringes	CO	4.41	5.46	4.99	0.31
	CO ₂	0.49	0.59	0.55	0.03
	OCN ⁻	0.15	0.23	0.20	0.03
	HCN, CH ₂ N ₂	3.53	4.28	3.90	0.29
	HNCO	0.55	0.58	0.56	0.01
<i>Residue (300 K) ($\times 10^{17}$ molecule cm^{-2})</i>					
2 fringes	CN groups	0.16	0.19	0.18	0.01
4 fringes	CN groups	0.40	0.44	0.42	0.01
6 fringes	CN groups	0.61	0.72	0.65	0.04

three molecules are equally present in the icy target. Thus the total amount of molecules that are traveled by the IR beam are approximately: 2.7×10^{18} molecules/ cm^2 (6 fringes), 1.8×10^{18} molecules/ cm^2 (4 fringes) and 1.0×10^{18} molecules/ cm^2 (2 fringes). The molecular column density refers, in this case, to a molecule having a mean molecular weight of 24 u (i.e. 1/3 of the sum of the molecular weights of CO, CH₄ and N₂).

As said the IR beam forms an angle of 45° with the plane of the sample. Wishing to evaluate the density of the deposited mixtures we need the column density that corresponds to the thickness of the sample. This can be obtained by multiplying the above values by the factor 0.833 obtained by knowing the incidence angle (45°) and the refractive index of the ice mixture (1.277, as measured at the wavelength of the laser from which the interference curve has been obtained). From these values and from the average thicknesses given above we can evaluate the density of the deposited mixtures: 0.68 g/ cm^3 (6 fringes), 0.67 g/ cm^3 (4 fringes) and 0.72 g/ cm^3 (2 fringes). The densities obtained for the three different thicknesses are the same within the experimental uncertainties that are mainly due to the procedure used to evaluate the column densities.

2.3. Ion bombardment induced chemical effects

Once deposited the icy mixtures have been irradiated with 200 keV He⁺ ion beams at a maximum dose of about 110 eV/16 u that is within the dosage scale required for the conversion of low molecular weight hydrocarbons into a refractory organic residue (Strazzulla and Johnson, 1991). We chose this dose as representative of the dose suffered by the external layers of comets and TNO by cosmic particles irradiation. In particular an outer web of devolatilized material, corresponding to a dosage of 100 eV/16 u, is developed down to substantial depths, for comets in the Oort clouds, for scattered TNOs and marginally for classical Kuiper's objects on time scales of the order of the age of the solar system (Strazzulla et al., 2003).

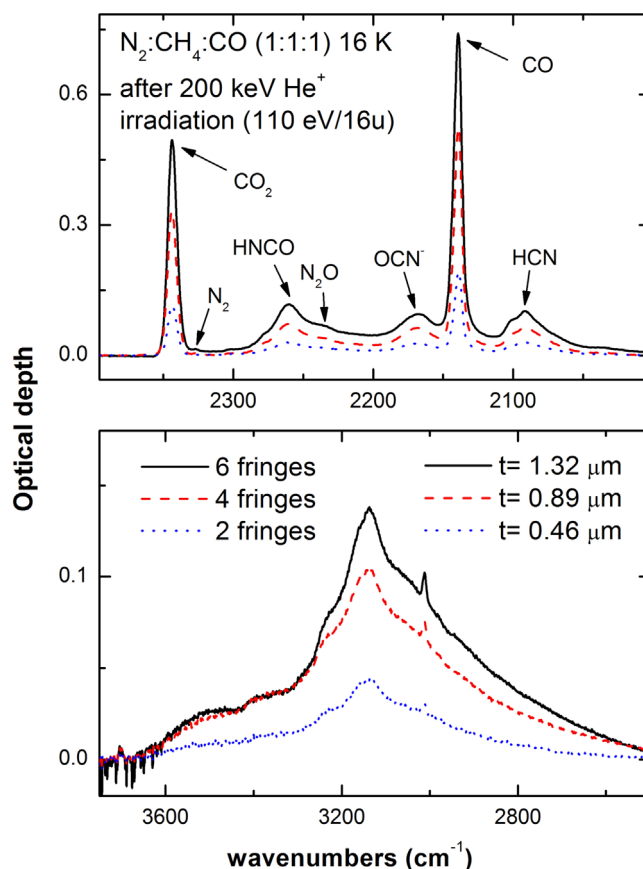


Fig. 3. Infrared spectra (16 K) of the icy mixtures N₂:CH₄:CO (1:1:1) after irradiation with 200 keV He⁺ ions (110 eV/16 u).

After some decades of experiments (e.g. Palumbo and Strazzulla, 1993; Baratta et al., 1994; Palumbo et al., 2008) it is well known that ion bombardment induces a series of effects among which chemical changes. This is made once more clear in Fig. 3 where the appearance of many bands (see Fig. 2 for comparison) testifies for the ion induced synthesis of several molecules. A multicomponent broad band observed between about 3600 and 2600 cm^{-1} (bottom panel of Fig. 3) is distinctive of the stretching vibrations of many C–H, O–H and N–H bearing molecules. We also see that the original CH₄ molecules are almost entirely destroyed to produce new species (e.g. Baratta et al., 2002; Garozzo et al., 2011). Particularly interesting is the spectral region between about 2400 and 2000 cm^{-1} (top panel of Fig. 3) where in addition to the remaining initial CO ($\sim 2140 \text{ cm}^{-1}$), several bands newly appear among which at: $\sim 2340 \text{ cm}^{-1}$ (CO₂), $\sim 2260 \text{ cm}^{-1}$ (HNCO), $\sim 2235 \text{ cm}^{-1}$ (N₂O), $\sim 2165 \text{ cm}^{-1}$ (OCN⁻), $\sim 2090 \text{ cm}^{-1}$ (HCN and CH₂N₂) (see e.g. Grim and Greenberg, 1987; Hudson et al., 2001; Palumbo et al., 2004; Sicilia et al., 2012). The carrier of the 2165 cm^{-1} band observed after UV photolysis and ion bombardment of interstellar ice analogs has been extensively debated in the astronomical literature. This feature was initially labeled XCN to indicate that it is due to the C≡N bond in an unknown (X) molecular species. It was then assigned to the cyanate ion OCN⁻ on the basis of several laboratory experiments on photolysis of interstellar ice analogs (e.g. Grim and Greenberg, 1987; Schutte and Greenberg, 1997; Demyk et al., 1998; Novozamsky et al., 2001). Alternatively, this feature is assigned to the C≡N group bonded in the refractory residues also formed after energetic processing of interstellar ice analogs (e.g. Palumbo et al., 2000a, 2000b, 2004; Materese et al., 2014). A weak feature, due to N₂, is also visible at 2328 cm^{-1} . The N₂ feature is not seen in the pristine ice and its appearance is probably due to the increased band strength of the

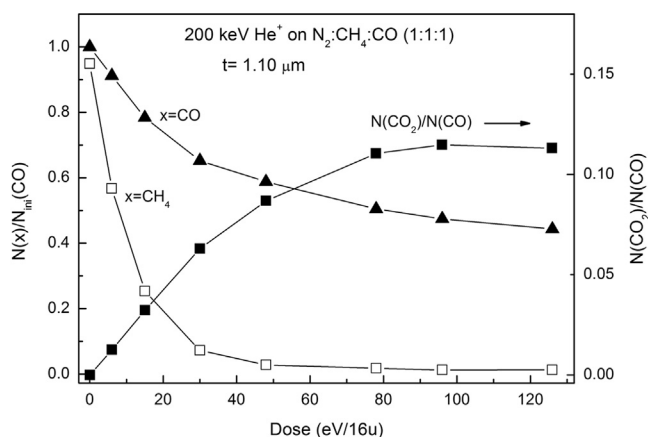


Fig. 4. CH_4 and CO normalized column densities and CO_2/CO column densities ratio of a 200 keV He^+ irradiated $\text{N}_2:\text{CH}_4:\text{CO}$ (1:1:1) mixture at different irradiation doses.

feature determined by the presence of CO_2 in the irradiated ice (Sandford et al., 2001). In addition to the features listed above, many other new features are present in the irradiated ice mixture below 2000 cm^{-1} at lower doses (10–40 eV/16 u), in particular: $\sim 1496\text{ cm}^{-1}$ (H_2CO), ~ 1466 and $\sim 1377\text{ cm}^{-1}$ (C_2H_6), ~ 1436 and $\sim 951\text{ cm}^{-1}$ (C_2H_4), $\sim 1089\text{ cm}^{-1}$ (HCO). Further information on the complex chemistry induced by energetic processing of $\text{N}_2:\text{CH}_4:\text{CO}$ ice mixtures can be found elsewhere (i.e. Hudson et al., 2001; Palumbo et al., 2004; Matarese et al., 2014); here we aim to characterize the organic residues produced by a relatively high irradiation dose of this mixture. Nevertheless it is interesting to note the different behaviors of the CH_4 and CO molecules upon irradiation: the first is almost completely lost, the second remains rather abundant (about 1/2, see Table 2).

This trend is clearly visible in Fig. 4 where the column densities of CH_4 and CO (both normalized to the initial column density of CO) and the ratio between the column densities of CO_2 and CO versus the dose are reported for a calibration experiment. This behavior is due to the fact the methane is easily decomposed in $\text{CH}_3 + \text{H}$, hydrogen escapes from the target and molecules having increasing C/H ratios are formed. Vice versa the main product of the CO radiolysis is CO_2 that, in turns, reforms CO when irradiated. In this way a quasi-equilibrium (steady-state) is reached in the CO/CO_2 ratio at least at the irradiation dose (110 eV/16 u) here investigated. The molecular column densities of CO_2 , OCN^- , $\text{HCN}-\text{CH}_2\text{N}_2$, HNCO and CO of the irradiated targets are reported in Table 2 that demonstrates the excellent reproducibility of the irradiated samples. Note that, in Table 2, we give the column density of $\text{HCN} + \text{CH}_2\text{N}_2$ since it is not possible to clearly distinguish the contribution of HCN and CH_2N_2 to the feature observed at 2090 cm^{-1} , in particular we adopted a single integrated band strength of $7.5 \pm 2.5 \times 10^{-18}\text{ cm molecule}^{-1}$ obtained as average of the HCN and CH_2N_2 band strengths. From Table 2 it is evident that the 56% of the initial amount of C atoms is present in the 6f films after irradiation. A contribution to this difference could be due to sputtering. Here we assume a quadratic dependence of the sputtering yield on the electronic stopping power (Se) and a $(\cos\theta)^{-1.67}$ dependence on the angle to the normal (Johnson, 1998). By considering the stopping power of 200 keV He^+ computed by TRIM software (Ziegler et al., 2008) and the erosion yields found in the literature for fast Helium ions on N_2 (Fig.11, Brown and Johnson, 1986), CO (Fig.12, Brown and Johnson, 1986) and CH_4 (Table 1, Johnson et al., 1983) we obtain: $Y(\text{N}_2)=35\text{ molecules/ion}$, $Y(\text{CO})=113\text{ molecules/ion}$ and $Y(\text{CH}_4)=213\text{ molecules/ion}$ for our experimental condition. In first approximation, in a mixture the yield for each species is proportional to its bulk concentration (Johnson, 1998) i.e. 1/3 of the pure ice yield for N_2 , CH_4 and CO . Since the bulk chemical

composition of the irradiated target changes upon irradiation, this approximation is valid only at very low dose. In particular most of the CH_4 molecules have already been converted into higher molecular weight species at a dose of 50 eV/16 u. Nevertheless a rough estimation of the possible amount of the eroded molecules can be obtained by assuming that the bulk composition does not change during irradiation. In particular we found that 3×10^{16} , 1.8×10^{17} and 9.8×10^{16} molecules cm^{-2} of N_2 , CH_4 and CO respectively would have been eroded at the end of irradiation in the 6f film, i.e. 15% of carbon atoms are eroded from the film. The thickness of the irradiated ice film can be in principle derived by looking at the variation of the fringes observed in the transmittance spectra. In particular if the refractive index of the film n is less than the refractive index of the substrate, as it is in our case, the thickness d of the film can be obtained through the formula:

$$d = \frac{1}{2n\nu_{\min} \sqrt{1 - \frac{\sin^2\theta_i}{n^2}}} \quad (1)$$

where ν_{\min} is the wavenumber of the zero order minimum and θ_i is the incidence angle. The equation can be solved to compute the thickness once the refractive index has been evaluated. The refractive index n of a 6f ice in the infrared at the wavenumber of the zero order minimum can be evaluated by substituting the thickness, measured by laser interference, in Eq. (1). In particular we obtain for a typical 6f ice film ($d=1.298\text{ }\mu\text{m}$, $\nu_{\min}=3652\text{ cm}^{-1}$) $n=1.27$. After a dose of 68 eV/16 u, we measure in the irradiated film $\nu_{\min}=4295\text{ cm}^{-1}$ that provide a thickness $d=1.104\text{ }\mu\text{m}$. In this computation we are assuming that the refractive index of the irradiated ice does not change. As a matter of fact, the refractive index of the ice film increases during irradiation, indeed at the highest dose of 110 eV/16 u, no interference fringes can be seen in the infrared spectrum indicating that n approached the refractive index n_2 of the MgF_2 substrate in the infrared i.e. $n_2=1.367$ ($\nu=4200\text{ cm}^{-1}$). By assuming that the thickness decreases linearly in the investigated dose range, we obtain at 110 eV/16 u, a thickness $d=0.984\text{ }\mu\text{m}$ i.e. a decrease of 16% in the thickness. This percentage is pretty similar to the amount of eroded C atoms estimated above. By considering that about 16% of the 6 fringes ice film has been eroded at the highest dose, most of the carbon ($\sim 70\%$) is accounted for after irradiation in Table 2. It should be considered that Table 2 does not includes the CH bearing molecules that contribute to the broad feature between 2600 and 3600 cm^{-1} . These molecules cannot be accounted for by IR spectroscopy since they cannot be distinguished from the OH and NH bearing species that also contribute to the broad $2600\text{--}3600\text{ cm}^{-1}$ feature.

2.4. The refractory organic residues

Once irradiated at 16 K, the sample is gently warmed up by switching off the cryostat, and left under vacuum overnight. The day after it is extracted from the chamber where a new MgF_2 window is lodged. In Fig. 5 we show two MgF_2 windows: one before it is put in the chamber and one after the processing where a brown material is clearly evident: it is the refractory material left over by ion bombardment of the icy mixtures. In the same figure the sample holder used to ship the windows to us and back to the LISA (Paris, France) Laboratory for their fitting in the flight module is shown.

The room temperature IR spectra of the residues have been obtained and are shown in Fig. 6. In the figure we have used the labels OR-6f, OR-4f and OR-2f to indicate the organic residue obtained from the 6 fringes, 4 fringes and 2 fringes ice films respectively. The spectra have been acquired after extraction of the

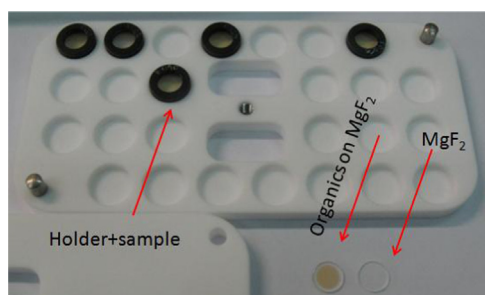


Fig. 5. Two MgF_2 windows are shown one as received and one after the processing where a brown residue is clearly evident. The sample holder used to ship the windows to us and back to the LISA Laboratory for their fitting in the flight module is also shown.

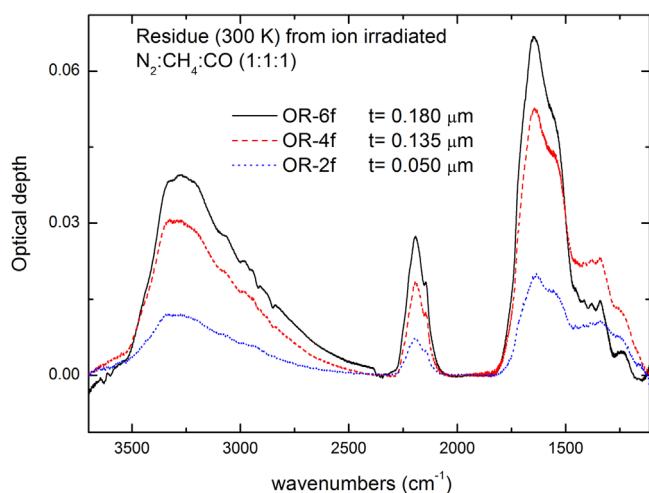


Fig. 6. IR spectra of the organic residues obtained after ion irradiation of the icy mixtures. The labels OR- x f indicate the organic residues obtained from x fringes ice films respectively; t is the actual thickness of the residues.

residues from the vacuum chamber, no significant change has been noticed with respect to the spectrum acquired in situ, before extraction, with the residue still under vacuum. It should be considered that volatile species present in the irradiated ice (i.e. CO , CO_2 , N_2 etc.) sublime during the slow warm up to room temperature, as a consequence the thickness decreases consistently in the organic residues as it is shown in the next.

We see that a lot of features are clearly present. A very broad band is observed between about 3600 and 2400 cm^{-1} . This band is distinctive of the stretching vibrations of many C–H, O–H and N–H bearing molecules and results from the sublimation of the residual volatiles still present after ion irradiation (see Fig. 3), from further chemical reactions induced by heating and from the physical re-arrangement of the structure of the material. The bending modes of the same groups and the stretching modes of C=O groups are evident in the spectral region 1800 – 1000 cm^{-1} . Also in this case, no quantitative estimation of the C–H nor the C=O stretching bearing molecules can be made by IR spectroscopy since they cannot be clearly distinguished from the other species that also contribute to the 3600 – 2400 and 1800 – 1000 cm^{-1} regions respectively. Particularly interesting is the multi-peaked band that is centered at about 2200 cm^{-1} and is distinctive of CN double and triple bonds. We have calculated the column density of the carrier of this band for all of the thirty samples (by using the same value of the band strength as used for OCN^-). The results are reported in Table 2 from which we can see, once again, the pretty good reproducibility of the samples.

More complex, less abundant species, could be present in the organic residue but have not been detected by IR spectroscopy. As an example, ion irradiation of nitrile (CH_3CN) containing ices has revealed the presence, in the organic residues, of complex molecules such as succinonitrile ' $\text{NCCH}_2\text{CH}_2\text{CN}$ ', 3-aminocrotonitrile ' $(\text{CH}_3)\text{C}(\text{NH}_2)\text{CHCN}$ ' etc.; these low abundance but astrobiologically relevant radiation products have been identified by gas chromatography–mass spectroscopy (GC–MS), where they are difficult to impossible to identify by classical IR spectroscopy alone (Hudson et al., 2008). By comparing the results obtained for other processed ice mixtures i.e.: far-UV photolysis of $\text{H}_2\text{O}:\text{CH}_3\text{OH}:\text{NH}_3:\text{HCN}$ (Bernstein et al., 2002), far-UV photolysis of $\text{H}_2\text{O}:\text{CH}_3\text{OH}:\text{NH}_3:\text{CO}:\text{CO}_2$ (Muñoz Caro et al., 2002), far-UV photolysis of $\text{H}_2\text{O}:\text{CH}_3\text{OH}:\text{NH}_3$ (Nuevo et al., 2006), 1.5 MeV H^+ radiolysis of $\text{H}_2\text{O}:\text{CH}_4:\text{NH}_3$ (Kobayashi et al., 1995) and their results (0.8 MeV H^+ radiolysis of $\text{H}_2\text{O}:\text{CH}_3\text{CN}$), Hudson et al. (2008) suggested that energetic processing of almost any organic ice containing C,H,N and O atoms probably results in formation of amino acid precursor that can be hydrolyzed to give the amino acids themselves. Recently a far-UV photolysis experiment of a $\text{N}_2:\text{CH}_4:\text{CO}$ (100:1:1) ice mixture has been presented (Matarese et al., 2014). The authors found that the IR spectrum of the organic residue obtained from the photolysed ice mixture is remarkably similar to the spectra of the residue obtained from 30 keV He^+ radiolysis of a $\text{H}_2\text{O}:\text{CH}_4:\text{N}_2$ (1:1:1) (Strazzulla et al., 2001) and a $\text{N}_2:\text{CH}_4:\text{CO}$ (1:1:1) ice mixtures (Palumbo et al., 2004) that is the same mixture considered in this work. Materese et al. (2014) suggested that the residues contain similar functional groups regardless differences in the energy source, the composition of the exact starting ice component and their respective relative abundances. GC–MS analysis of the far-UV photolysed organic residue reveals the presence of many complex molecules i.e. glyceric acid ($\text{C}_3\text{H}_6\text{O}_4$), lactic acid ($\text{C}_3\text{H}_6\text{O}_3$), urea ($\text{CH}_4\text{N}_2\text{O}$) etc. (Materese et al., 2014). Hence, even if IR spectroscopy does not detect them due to its relatively low sensitivity (Hudson et al., 2008; Materese et al., 2014), astrobiologically relevant complex molecules are probably present in the organic residues described in this work.

For the residues we have also obtained the transmittance spectra in the 0.2 – $2.5\text{ }\mu\text{m}$ ($50,000$ – 4000 cm^{-1}) range, by using a Lambda 19 Perkin Elmer dispersive spectrometer. As an example, in Fig. 7 we show the composite transmittance spectrum in the full range (0.2 – $10\text{ }\mu\text{m}$; $50,000$ – 1000 cm^{-1}) for a sample obtained after ion bombardment of the thickest ice sample (six fringes).

Note that the spectrum between 1.3 and $10\text{ }\mu\text{m}$ is the same shown in Fig. 6 after the subtraction of the continuum and in an

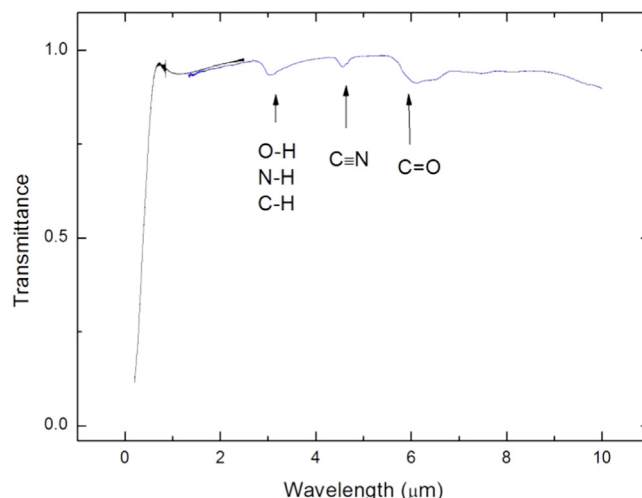


Fig. 7. Composite transmittance spectrum for a sample obtained after ion bombardment of the thickest ice sample (six fringes).

optical depth scale. The spectrum exhibits a local minimum at about $1.18 \mu\text{m}$, due to the interference, in the transmittance spectra. By using the formulas given in Sreemany et al. (2004) at normal incidence (for $n_0 < n$, $n > n_2$) we obtain:

$$\frac{T_{\max}}{T_{\min}} = \frac{(n_0 n_2 + n^2)^2}{(n_0 + n_2)^2 n^2} \quad (2)$$

where $n_0=1$ (refractive index of the medium) and $n_2=1.374$ (refractive index of the MgF_2 substrate at $\lambda=1 \mu\text{m}$), we can evaluate the refractive index n from the maximum to minimum ratio (T_{\max}/T_{\min}) in the transmittance average spectrum obtained by considering all the thickest (6 fringes) samples. In particular we obtained at $\lambda_{\min}=1.18 \mu\text{m}$ a refractive index $n=1.58$. Hence, by using the equation given in Sreemany et al. (2004), the thickness of the film can be computed through the equations:

$$nd = \left[\frac{1}{4}(2m + 1) \lambda_{\min} \right] \text{ for minimum} \quad (3a)$$

$$nd = \left[\frac{1}{4}(2m + 2) \lambda_{\max} \right] \text{ for maximum} \quad (3b)$$

in the equations d is the thickness, n is the refractive index of the film, $m=0,1,2,\dots$ is the order of the minimum/maximum. It should be considered that if $n_0 < n < n_2$ (as it was for the as deposited ices) Eqs. (3a) and (3b) become valid for maxima and minima respectively. In our case, by substituting $m=0$, $\lambda_{\min}=1.18 \mu\text{m}$ and $n=1.58$ in Eq. (3a) we obtain an average thickness of $\sim 0.187 \pm 0.005 \mu\text{m}$. Also in this case the reproducibility of the thickness of the 10 residues obtained from the thickest samples is high (standard deviation=4%), by looking at the scatter in the minimum positions of the corresponding UV–vis–NIR transmittance spectra. The average thickness obtained in this way has been used as initial approximation for a more accurate computation that has been used to evaluate the optical constants of the organic residue. For this purpose, the range covered by our spectra (0.200–10 μm) has been extended in the far UV by acquiring the spectra of all the 30 samples in the vacuum UV range, down to $0.119 \mu\text{m}$, at LISA (Paris, France) using a Horiba Jobin Yvon VUV H20–UJL monochromator (Saiagh et al., 2014). The average transmittance spectra obtained for the considered thicknesses are reported in Fig. 8.

The range of computation of the optical constants has been also extended at longer wavelength (20 μm) by considering the IR

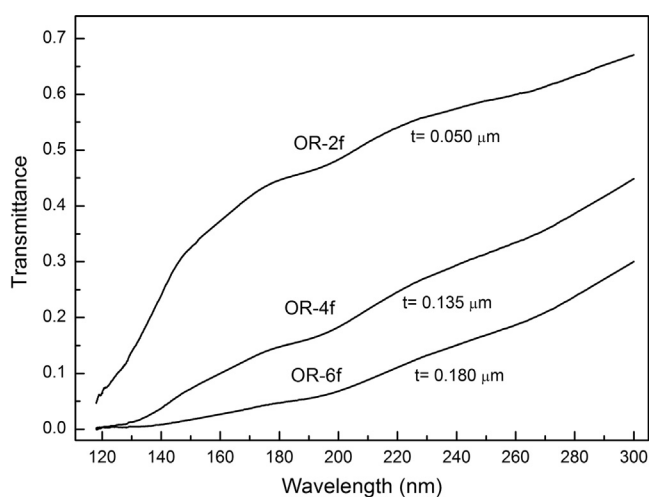


Fig. 8. Average transmittance spectra of the organic residues in the FUV range acquired at LISA. The labels OR-xf indicate the organic residues obtained from x fringes ice films respectively; t is the actual thickness of the residues.

spectra obtained for an organic residue produced on a KBr substrate by following the same experimental procedure used for the other, on MgF_2 substrate, samples. In particular we obtained a Kramers–Kronig constrained set of optical constants as the best fit solution to the experimental MIR and UV–vis–NIR transmission spectra together with the average best fit thicknesses of the residue obtained from six ($0.180 \mu\text{m}$), four ($0.135 \mu\text{m}$), two ($0.050 \mu\text{m}$) and a single 5 ($0.148 \mu\text{m}$, on KBr) fringes ice samples. The method of the Kramers–Kronig constrained variational dielectric function fitting (KKCVDF) was employed (Kuzmenko, 2005). We individuate two separate fitting region ($1850\text{--}84,000 \text{cm}^{-1}$) and ($500\text{--}1850 \text{cm}^{-1}$) for the MgF_2 and KBr substrate organic residues respectively. For the optical model of the transmittance of the film plus substrate system, we consider the film as ‘thin’ and the substrates as ‘thick’. In particular, in the ‘thin’ case the waves reflected successively at the interface film–vacuum and film–substrate add coherently (interference is observed). On the other hand the substrate can be usually considered thick since its depth is much greater than the wavelength; so variations in the flatness and parallelism of the two surfaces will be appreciable fractions of a wavelength. Under these conditions no interference effect can be observed in the substrate. Hence the waves reflected successively at the front (with film) and back surface add incoherently. In this latter case the resultant is the sum of the various intensities regardless of their phases. All the optical calculations and fitting procedures have been carried out by using a computer code called REFFIT, this code implement the KKCVDF technique and is available online (Kuzmenko, 2004). As an example, in Fig. 9 is reported the comparison between the theoretical fitting spectra and the average experimental spectra, of all the organic residues on the MgF_2 substrates, for the three considered thicknesses.

A particular of the comparison between the theoretical and experimental spectra in the IR region is reported in Fig. 10.

From the comparison it is evident that the ability of the optical constants to reproduce the experimental transmission spectra for all the considered thicknesses and substrates is good.

The computed optical constants are reported in Fig. 11 and are available online at the following link: (<http://www.oact.inaf.it/weboac/labsp/ORPSS.html>).

In a separate experiment we prepared a residue on a quartz micro-balance following the same procedure as used to prepare the thickest residues on MgF_2 windows. The frequency variation of the balance corresponded to a deposited mass per unit area of

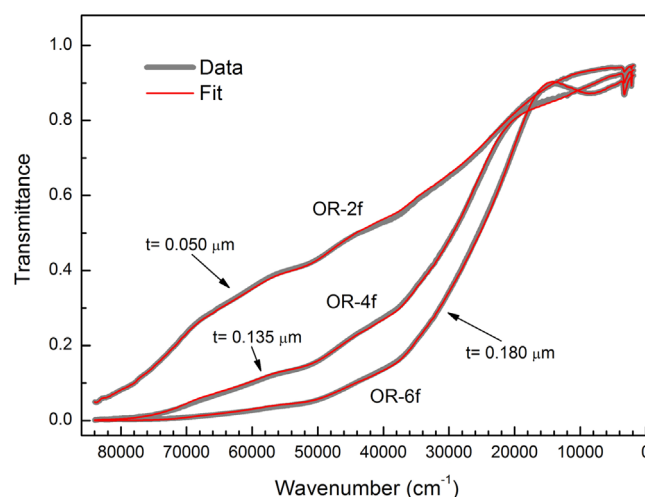


Fig. 9. Comparison between theoretical (fit) and experimental average spectra of the organic residues on MgF_2 substrate. The labels OR-xf indicate the organic residues obtained from x fringes ice films respectively; t is the actual thickness of the residues.

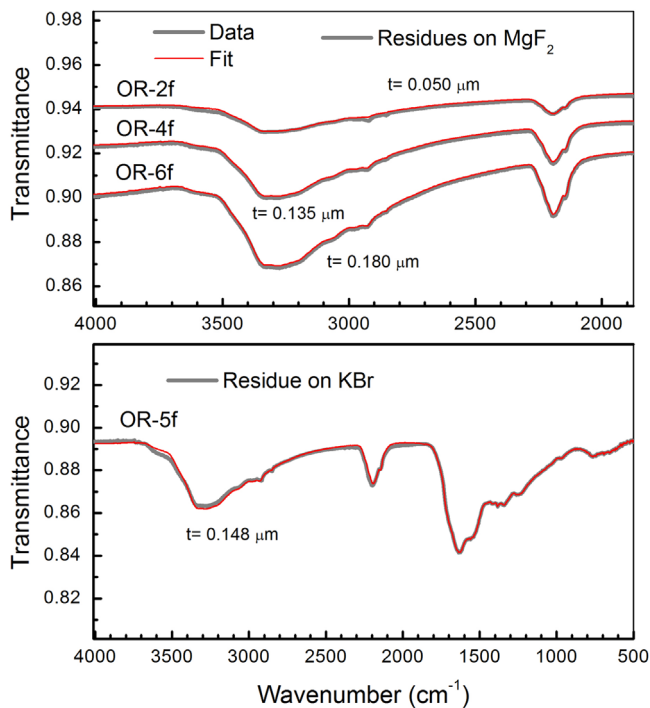


Fig. 10. Comparison between theoretical (fit) and experimental average spectra of the organic residues on MgF₂ and KBr substrates in the IR range. The labels OR-xf indicate the organic residues obtained from x fringes ice films respectively; t is the actual thickness of the residues.

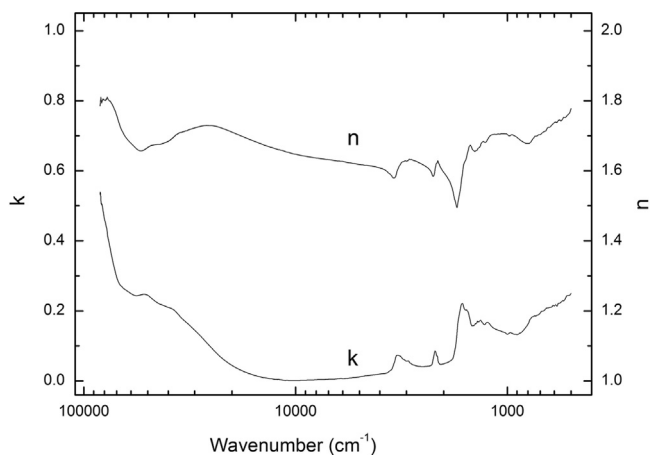


Fig. 11. Optical constants of the organic residue.

$2.09 \times 10^{-5} \text{ g/cm}^2$. The density of the residues is then $(1.17 \pm 0.02) \text{ g/cm}^3$.

3. Discussion and perspective

We have described the preparation and the physico-chemical characterization of organic samples that will be exposed to solar electromagnetic radiation for several months, on board of the International Space Station (ISS). What is important to outline is why we wish to expose those materials and which are the foreseen information we will obtain.

As said the icy mixtures (N₂:CH₄:CO) that have been irradiated are well representative of ices present on the surfaces of Trans Neptunian Objects (TNO) and of comets in the Oort cloud. Moreover cosmic ion bombardment is believed to be a relevant agent to induce the physico chemical processing of those surfaces. Thus

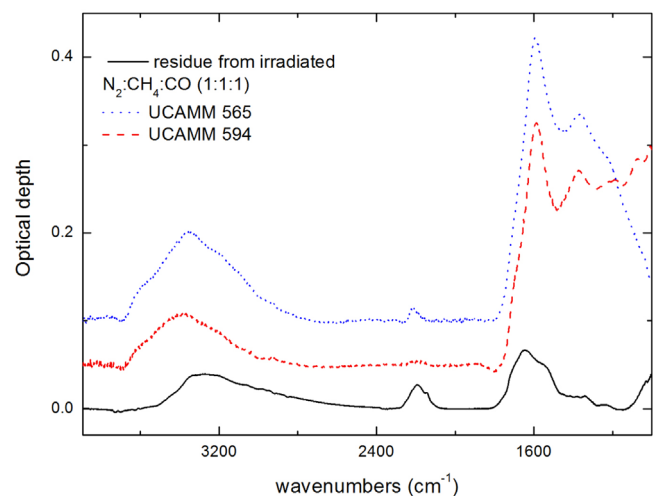


Fig. 12. Comparison of the IR spectra of one of our residue with those of two ultracarbonaceous Antarctic meteorites (courtesy of E. Dartois and C. Engrand).

materials similar to the ones synthesized in the laboratory after bombardment at low temperature (whose spectra are shown in Fig. 3) are expected to be present on those surfaces.

When comets arrive in the proximity of the Sun their surfaces are heated and the water dominated sublimation expels gas and dust. Organic refractory materials, similar to those we have synthesized, are believed to be a component of the cometary dust.

These materials travel the interplanetary medium where they are further processed because of the exposure to the solar corpuscular and electromagnetic radiation. We wish to investigate such a processing by exposing our organic residues to the solar radiation.

To better clarify the goal of the experiment we show, in Fig. 12, a comparison of the IR spectra of one of our residue with those of two ultracarbonaceous Antarctic meteorites (Dartois et al., 2013) thought to have been originated in the outer solar system at temperatures as low to allow the condensation of nitrogen. The comparison shows that the laboratory sample does not fit the two spectra of meteorites (that are different themselves) but exhibit however similar bands having different ratios of the organic groups responsible for each component of multi-peaked bands. These differences could be due to a different composition of the parent molecules or to a different processing of the organic materials or both. With the present planned experiments on the ISS we wish to give a contribution to the field by studying how the spectra of the exposed samples will vary.

As said we have prepared a total of 30 samples having three different thicknesses (10 samples for each thickness). For each thickness 4 of the 10 samples are flying (two exposed to solar UV photons+GCR+temperature cycling, and two, arranged below, to GCR+temperature cycling) and six have been delivered to a DLR facility in Cologne: two will be saved in vacuum and subjected to the same temperature variations (on the order of 50 °C) as in the ISS by telemetry, two are subjected to the same temperature variations and additionally exposed to visible and near UV irradiation by a solar simulator; and two are saved in vacuum at 5 °C (see Cottin et al., 2015a, 2015b for further details).

After exposure, all of the samples will be then sent in our laboratory where the spectroscopic analysis of the 30 samples will be performed and compared with those here described. The comparison between the samples aboard of the ISS (exposed and not exposed to solar UV) and the samples at DLR will help to separate the contributions of GCR (that, as shown in the next is expected to be negligible), solar UV photons and temperature variations in modifying the spectra of the exposed samples.

The samples that we expect to exhibit the largest spectral variations are those exposed to solar UV photons. The expected temperature excursion outside ISS is limited ($\sim 50^\circ\text{C}$) and the samples are refractory enough (Palumbo et al., 2004); hence we do not expect large spectral variations due to the temperature cycling. However we are studying in our laboratory the evolution, with time, of the spectra of our residues left at room T and the comparison of the flying samples with the laboratory ones will clarify the point.

The exposed sample is in the internal face of the MgF_2 thus they are irradiated by solar electromagnetic radiation (including ionizing vacuum UV solar photons) and energetic cosmic ions (e.g. protons having energies greater than about 15 MeV) that can penetrate the windows (about 1 mm thick). We expect that the maximum effect will be given by vacuum UV photons that will be not used in the DLR laboratories with the solar simulator. The comparison between the samples exposed to the solar UV photons outside ISS and the samples exposed to the solar simulator at DLR will help providing information on the contribution of the more energetic vacuum UV solar photons (below 200 nm) to modify the samples.

Additional experiments are planned in our laboratory by using an UV lamp (mostly emitting Ly-alpha photons) and irradiating additional samples identical to those here described.

In fact previous laboratory experiments show that the $\text{C}\equiv\text{N}$ bonds are permanent at room temperature, but are destroyed by further ion irradiation (Palumbo et al., 2004). Then their exposure to interplanetary space environments in the EXPOSE-R2 facility on board ISS will allow analysis of their destruction and evaluation of their lifetime in the interplanetary medium.

What will be the total irradiation dose suffered by our residues outside the ISS? Based on the results obtained for the previous Expose-R mission experiment AMINO (Cottin et al., 2015a), we give an estimation in the next paragraph.

AMINO samples have been exposed for 682 days (1 year and 10 months). The samples were not always facing the Sun because ISS orbits around Earth and adopts various orientations relative to the Sun. In addition multiple shadows by solar panels and the ISS environments in the vicinity of the Expose-R facility (radiators etc.) significantly decrease the effective insulation. The orientation of the ISS has been reconstructed and the insulation on the Expose-R has been modeled. Results from this computation, adjusted with measurements from detectors embedded in the Expose-R facility, gave an average, over the whole duration of the mission, equivalent to perpendicular solar irradiation at 1 AU of 130 h/month (Cottin et al., 2015a). The same procedure will be followed for the PSS experiment when the mission will be over, for the time being, we assume that our samples will experience the same average insulation. The scheduled exposure duration for PSS experiment is actually of 16 months; hence a total equivalent perpendicular solar illumination of 2080 h is expected. The fraction of solar UV photons absorbed by our residue ($\text{ads}(\lambda)$) can be approximated by the relation: $\text{ads}(\lambda) = (1 - e^{-\alpha(\lambda)x})$, where x is the thickness of the film and the absorption coefficient $\alpha(\lambda) = 4\pi k(\lambda)/\lambda$. In the previous relation $k(\lambda)$ is equal to the extinction coefficient k of the optical constants computed for our samples. By considering the ASTM E-490 standard solar spectrum, the density of our residue and the transmittance of the MgF_2 window, we obtain an irradiation dose rate for the OR-2f organic residue ($x=50$ nm) of $0.7 \text{ eV}/16 \text{ u h}^{-1}$ over the ($119.5 < \lambda < 206.7$ nm) range. Hence a total UV irradiation dose of $0.7 \text{ eV}/16 \text{ u h}^{-1} \times 2080 \text{ h} = 1460 \text{ eV}/16 \text{ u}$ is expected for the OR-2f (50 nm) residue. The thicker samples, OR-4f ($x=135$ nm) and OR-6f ($x=180$ nm) will be irradiated at a lower average dose since UV photons are absorbed through the film. By following the method described in Baratta et al. (2002), it will be possible, after exposure to the UV solar photons,

to compute the transmittance of the organic residues at different depths i.e. at lower irradiation doses. In the following we indicate with T_{OR2f} , T_{OR4f} and T_{OR6f} the transmittance of the exposed OR-2f, OR-4f and OR-6f organic residues respectively. The transmittance of the slab at a depth between 50 and 135 nm, given by $T_{\text{OR4f-2f}} = T_{\text{OR4f}}/T_{\text{OR2f}}$ Baratta et al. (2002), will correspond to a total irradiation dose of 520 eV/16 u and the transmittance of the slab at a depth between 135 and 180 nm, given by $T_{\text{OR6f-4f}} = T_{\text{OR6f}}/T_{\text{OR4f}}$, will correspond to a total irradiation dose of 164 eV/16 u. It should be considered that the average irradiation dose at depth could be lower if the solar UV photons cause a further darkening of the organic residue.

For the AMINO experiment, the energetic particles environments were measured by the 3RD-R experiment behind a shielding of 0.4 g/cm^2 which is similar to the shielding provided by the MgF_2 windows of 0.31 g/cm^2 . The average dose of particles was calculated to $84 \mu\text{Gy/day}$ for GCR, $506 \mu\text{Gy/day}$ for South Atlantic Anomaly (SAA) protons and $89 \mu\text{Gy/day}$ for Outer Radiation Belt (ORB) electrons (Cottin et al., 2015a). If we assume that the average dose rate will be the same for the PSS experiment, we obtain a dose of 50 mGy from GCR, 273 mGy for SAA protons and 48 mGy for ORB. Hence a total irradiation dose of 371 mGy is expected for our residues by energetic particles. This dose corresponds to $6 \times 10^{-8} \text{ eV}/16 \text{ u}$, that will give negligible chemical effects with respect to the UV irradiation dose, in our residues. We hope, with these experiments, to give a further contribution on the debate on the relevance that material coming from space has for the chemical evolution of Earth and other objects in the solar system and beyond.

Acknowledgments

This research has been supported by the Italian Space Agency (ASI) contract no. 2013-073-R.0: PSS (Photochemistry on the Space Station). H.C. acknowledges support by the Center National d'Etudes Spatiales (CNES). Diana Khalaf contributed to the measurements of VUV spectra of the samples.

References

- Baratta, G.A., Castorina, A.C., Leto, G., Palumbo, M.E., Spinella, F., Strazzulla, G., 1994. *Planet. Space Sci.* 42, 759.
- Baratta, G.A., Palumbo, M.E., 1998. *J. Opt. Soc. Am. A* 15, 3076.
- Baratta, G.A., Leto, G., Palumbo, M.E., 2002. *Astron. Astrophys.* 384, 343.
- Bernstein, M.P., Dworkin, J.P., Sandford, S.A., Cooper, G.W., Allamandola, L.J., 2002. *Nature* 416, 401.
- Bernstein, M.P., Sandford, S.A., Allamandola, L.J., 1997. *Astrophys. J.* 476, 932.
- Brown, W.L., Johnson, R.E., 1986. *Nucl. Instrum. Methods Phys. Res. B* 13, 295.
- Brunetto, R., Barucci, M.A., Dotto, E., Strazzulla, G., 2006. *Astrophys. J.* 644, 646.
- Cooper, J.F., Christian, E.R., Richardson, J.D., Whang, C., 2003. *Earth Moon Planets* 92, 261.
- Cottin, H., Saïagh, K., Guan, Y.Y., Cloix, M., Khalaf, D., Macari, F., Jérôme, M., Poliendor, J.-M., Bénilan, Y., Coll, P., Fray, N., Gazeau, M.-C., Raulin, F., Stalport, F., Carrasco, N., Szopa, C., Bertrand, M., Chabin, A., Westall, F., Vergne, J., Da Silva, L.A., Maurel, M.C., Chaput, D., Demets, R., Brack, A., 2015a. *Int. J. Astrobiol.* 14, 67.
- Cottin, H., Saïagh, K., Nguyen, D., Grand, N., Bénilan, Y., Cloix, M., Coll, P., Gazeau, M.-C., Fray, N., Khalaf, D., Raulin, F., Stalport, F., Carrasco, N., Szopa, C., Chaput, D., Bertrand, M., Westall, F., Mattiotta, A., Quinn, R., Ricco, A., Santos, O., Baratta, G., Strazzulla, G., Palumbo, M.E., Postollec, A.L., Dobrijevic, M., Coussot, G., Vigier, F., Vandenebeele-Trambouze, O., Incerti, S., Berger, T., 2015b. *Bull. Soc. R. Sci. Liège* 84, 60.
- Demyk, K., Dartois, E., d'Hendecourt, L., Juordain de Muizon, M., Heras, A.M., Breitfellner, M., 1998. *Astron. Astrophys.* 339, 553.
- Dartois, E., Engrand, C., Brunetto, R., et al., 2013. *Icarus* 224, 243.
- Fulvio, D., Sivaraman, B., Baratta, G.A., et al., 2009. *Spectrochim. Acta A* 72, 1007.
- Garozzo, M., La Rosa, L., Kanuchova, Z., Ioppolo, S., Baratta, G.A., Palumbo, M.E., Strazzulla, G., 2011. *Astron. Astrophys.* 528, A118.
- Guan, Y.Y., Fray, N., Coll, P., Macari, F., Raulin, F., Chaput, D., Cottin, H., 2010. *Planet. Space Sci.* 58, 1327.
- Grim, R.J.A., Greenberg, J.M., 1987. *Astrophys. J.* 321, L91–L96.
- Grundy, W.M., Buie, M.W., 2002. *Icarus* 157, 128.

- Jenniskens, P., Baratta, G.A., Kouchi, A., de Grot, M.S., Greenberg, M.J., Strazzulla, G., 1993. *Astron. Astrophys.* 273, 583.
- Jiang, G.J., Person, W.B., Brown, K.G., 1975. *J. Chem. Phys.* 62, 1201.
- Johnson, R.E., Lanzerotti, L.J., Brown, W.L., Augustyniak, W.M., Mussi, C., 1983. *Astron. Astrophys.* 123, 343.
- Johnson, R.E., 1998. *Solar System Ices*. In: Schimdt, B., et al. (Eds.), 1998. Kluwer Academic Publishers, Printed in the Netherlands, pp. 303–334.
- Hudson, R.L., Moore, M.H., Gerakines, P.A., 2001. *Astron. Astrophys. J.* 550, 1140–1150.
- Hudson, R.L., Moore, M.H., Dworkin, J.P., Mildred, P.M., Zachary, D.P., 2008. *Astrobiology* 8, 771.
- Kerkhof, O., Schutte, W.A., Ehrenfreund, P., 1999. *Astron. Astrophys.* 346, 990.
- Kobayashi, K., Kasamatsu, T., Kaneko, T., Koike, J., Oshima, T., Saito, T., Yamamoto, T., Yanagawa, H., 1995. *Adv. Space Res.* 16, 221.
- Kuzmenko, A.B., 2004. (<http://optics.unige.ch/alexey/refit.html>).
- Kuzmenko, A.B., 2005. *Rev. Sci. Instrum.* 76, 083108.
- Materese, C.K., Cruikshank, D.P., Sandford, S.A., Imanaka, H., Nuevo, M., White, D.W., 2014. *Astron. Astrophys. J.* 788, 111.
- Modica, P., Palumbo, M.E., 2010. *Astron. Astrophys.* 519, A22.
- Mulas, G., Baratta, G.A., Palumbo, M.E., Strazzulla, G., 1998. *Astron. Astrophys.* 333, 1025.
- Muñoz Caro, G.M., Meierhenrich, U.J., Schutte, W.A., Barbier, B., Arcones Segovia, A., Rosenbauer, H., Thiemann, W.H.P., Brack, A., Greenberg, J.M., 2002. *Nature* 416, 403.
- Novozamsky, J.H., Schutte, W.A., Keane, J.V., 2001. *Astron. Astrophys.* 379, 588.
- Nuevo, M., Meierhenrich, U.J., Muñoz Caro, G.M., Dartois, E., d'Hendecourt, L., Deboffle, D., Auger, G., Blanot, D., Bredehöft, J.H., Nahon, L., 2006. *Astron. Astrophys.* 457, 741.
- Owen, T.C., Roush, T.L., Cruikshank, D.P., et al., 1993. *Science* 261, 745.
- Palumbo, M.E., Strazzulla, G., 1993. *Astron. Astrophys.* 269, 568.
- Palumbo, M.E., Strazzulla, G., Pendleton, Y.J., Tielens, A.G.G.M., 2000a. *Astron. Astrophys. J.* 534, 801.
- Palumbo, M.E., Pendleton, Y.J., Strazzulla, G., 2000b. *Astron. Astrophys. J.* 542, 890.
- Palumbo, M.E., Ferini, G., Baratta, G.A., 2004. *Adv. Space Res.* 33, 49.
- Palumbo, M.E., Leto, P., Siringo, C., Trigilio, C., 2008. *Astron. Astrophys. J.* 685, 1033.
- Raulin, F., Bruston, P., Paillous, P., Sternberg, R., 1995. *Adv. Space Res.* 15 (3), 321.
- Saiagh, K., Cloix, M., Fray, N., Cottin, H., 2014. *Planet. Space Sci.* 90, 90.
- Sandford, S.A., Bernstein, M.P., Allamandola, L.J., Goorvitch, D., Teixeira, T.C.V.S., 2001. *Astron. Astrophys. J.* 548, 836.
- Shen, C.J., Greenberg, J.M., Schutte, W.A., van Dishoeck, E.F., 2004. *Astron. Astrophys.* 415, 203.
- Schutte, W.A., Greenberg, J.M., 1997. *Astron. Astrophys.* 317, L43.
- Sicilia, D., Ioppolo, S., Vindigni, T., Baratta, G.A., Palumbo, M.E., 2012. *Astron. Astrophys.* 543, A155.
- Sreemany, et al., 2004. *Mater. Chem. Phys.* 83, 169–177.
- Strazzulla, G., Cooper, J.F., Christian, E.R., Johnson, R.J., 2003. *C.R. Phys.* 4, 791.
- Strazzulla, G., Baratta, G.A., Palumbo, M.E., 2001. *Spectrochim. Acta Part A* 57, 825.
- Strazzulla, G., Baratta, G.A., 1992. *Astron. Astrophys.* 266, 434.
- Strazzulla, G., Johnson R.E., 1991. In: *Comets in the Post-Halley Era, ASSL Series*, Kluwer, Dordrecht, vol 1, p. 2.
- Szabó, Gy.M., Sárneczky, K., Kiss, L.L., 2011. *Astron. Astrophys.* 531, A11.
- Yamada, H., Person, W.B., 1964. *J. Chem. Phys.* 41, 2478.
- van Broekhuizen, F.A., Keane, J.V., Schutte, W.A., 2004. *Astron. Astrophys.* 415, 425.
- Vigier, F., Le Postollec, A., Coussot, G., Chaput, D., Cottin, H., Berger, T., Incerti, S., Triqueneaux, S., Dobrijevic, M., Vandenabeele-Trambouze, O., 2013. *Adv. Space Res.* 52, 2168.
- Ziegler, J.F., Ziegler, M.D., Biersack, J.P., 2008. *The Stopping and Range of Ions in Solids*. Pergamon Press, New York (<http://www.srim.org>).